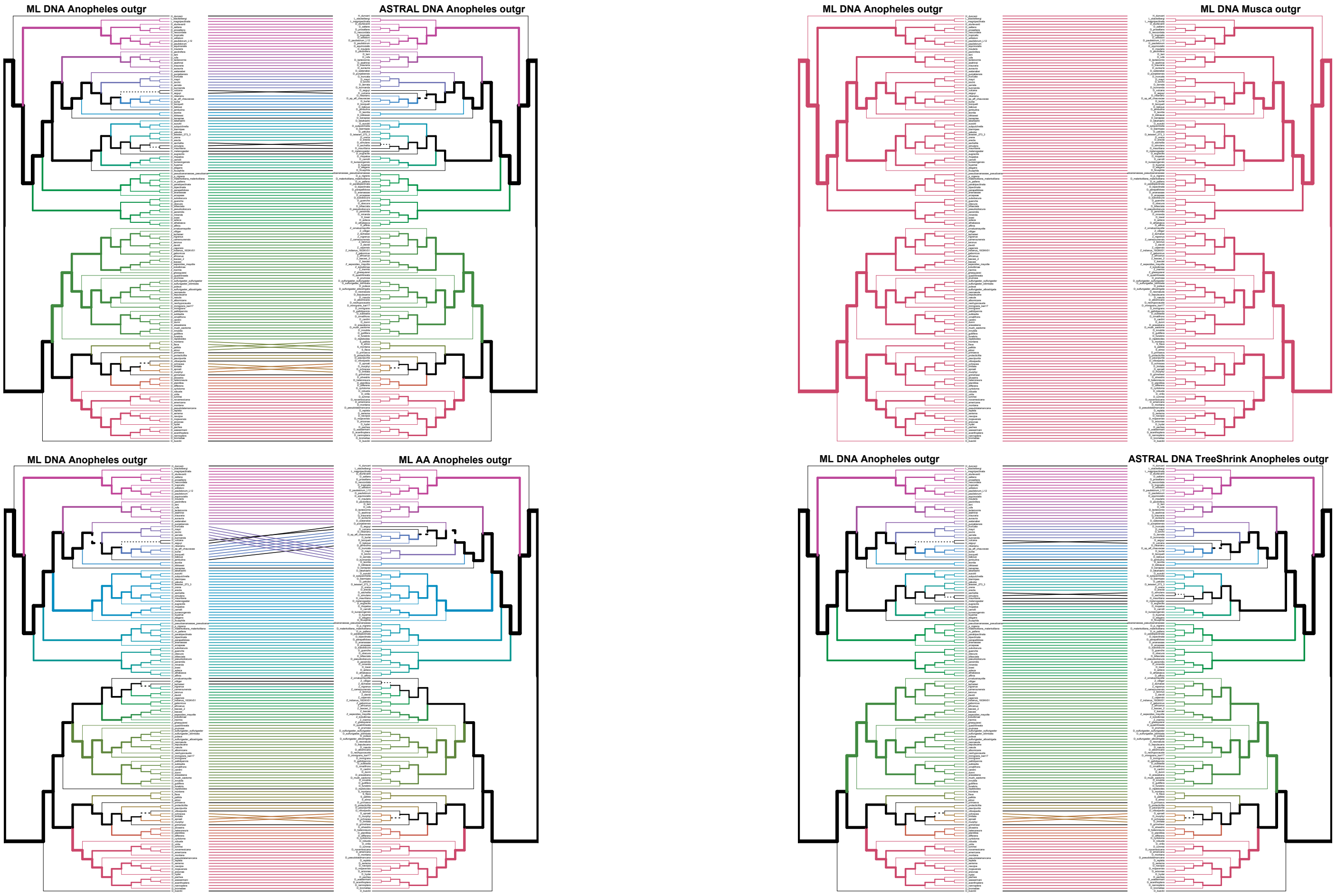

Figure S1. Topological comparisons between trees inferred by different methods, related to Figure 1. Black paths on the phylogenetic trees lead to dashed branches that indicate topological incongruencies.

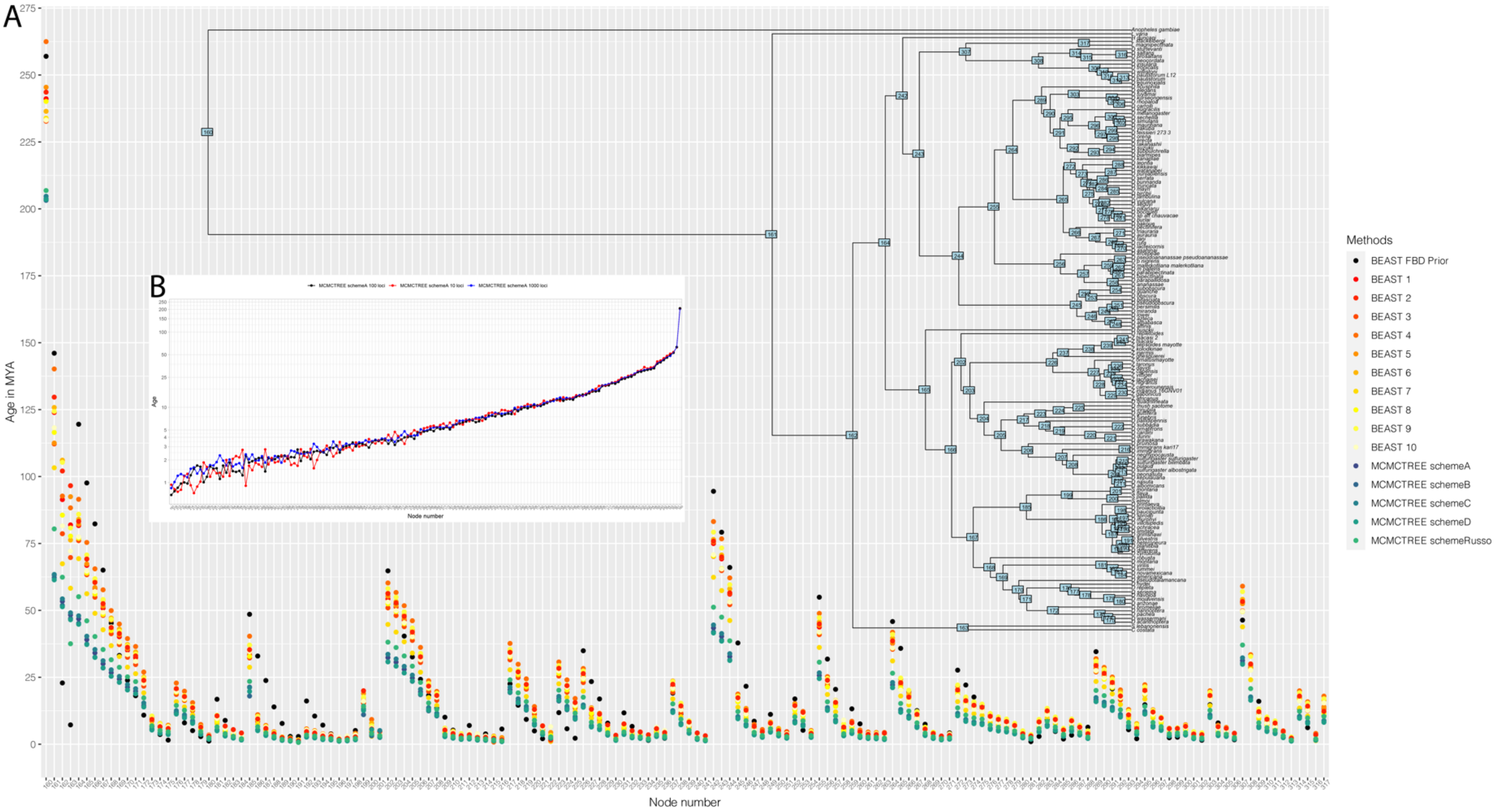

Figure S2. Divergence time estimation, related to Figure 1.
(A) Age estimates produced by different calibration schemes and methods. *x*-axis indicates node numbers. The *y*-axis represents the inferred age in MYA.
(B) Comparison between nodal calibrations based on different numbers of loci using scheme A. Nodes are arranged on the *x*-axis according to scheme A from the youngest to the oldest. The *y*-axis represents the log of inferred age in MYA.

4

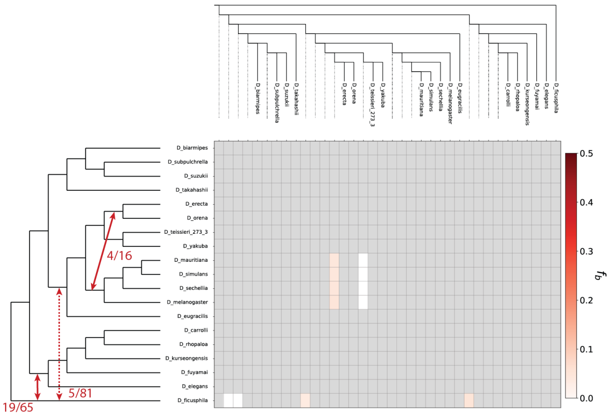
D_biarmipes
D_subpulchrella
D_suzukii
D_takahashii
D_erecta
D_orena
D_teissieri_273_3
D_yakuba
D_mauritiana
D_simulans
D_sechellia
D_melanogaster
D_eugracilis
D_carrolli
D_rhopaloa
D_kurseongensis
D_fuyamai
D_elegans
D_ficusphila
4/16
5/81
19/65
0.5
0.4
0.3
0.2
0.1
0.0
f_b

8

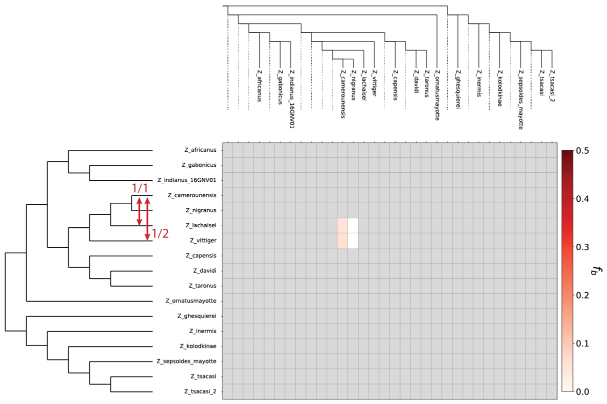
Z_africanus
Z_gabonicus
Z_indianus_16GNV01
Z_camerounensis
Z_nigranus
Z_lachaisei
Z_vittiger
Z_capensis
Z_davidi
Z_taronus
Z_ornatusmayotte
Z_ghesquierei
Z_inermis
Z_kolodkinae
Z_sepsoides_mayotte
Z_tsacasi
Z_tsacasi_2
1/1
1/2
0.5
0.4
0.3
0.2
0.1
0.0
f_b

5

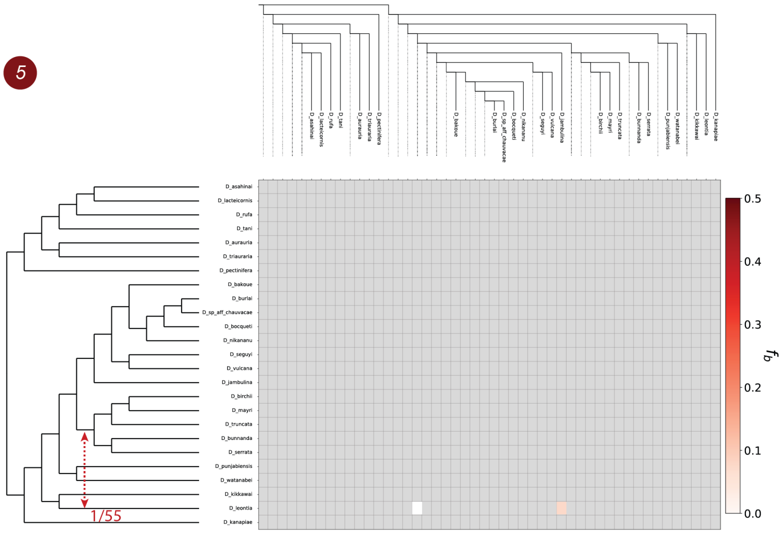
D_asahinai
D_lacteicornis
D_rufa
D_tani
D_auraria
D_triauraria
D_pectinifera
D_bakoue
D_burlai
D_sp_aff_chauvacae
D_bocqueti
D_nikananu
D_seguyi
D_vulcana
D_jambulina
D_birchii
D_mayri
D_truncata
D_bunnanda
D_serrata
D_punjabiensis
D_watanabei
D_kikkawai
D_leontia
D_kanapiae
1/55
0.5
0.4
0.3
0.2
0.1
0.0
f_b

6

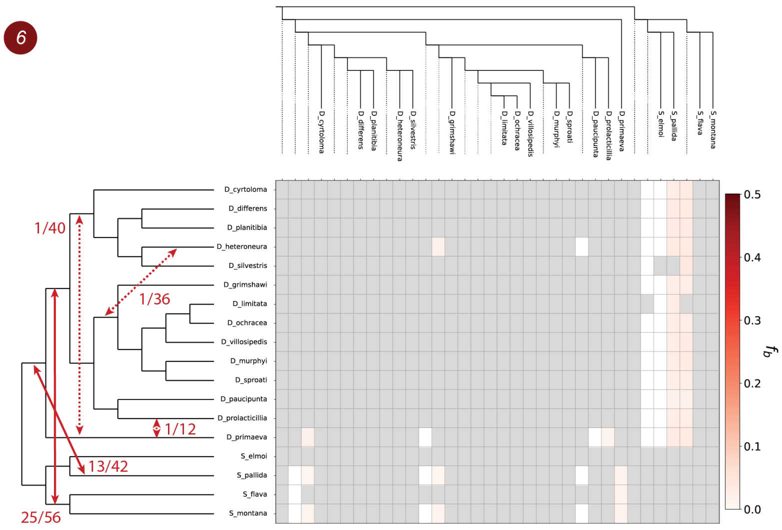
D_cyrtoloma
D_differens
D_planitibia
D_heteroneura
D_silvestris
D_grimshawi
D_limitata
D_ochracea
D_villosipedis
D_murphyi
D_sproati
D_paucipunta
D_prolacticillia
D_primaeva
S_elmoi
S_pallida
S_flava
S_montana
1/40
1/36
1/12
13/42
25/56
0.5
0.4
0.3
0.2
0.1
0.0
f_b

Figure S3. Patterns of introgression inferred for the monophyletic clades 4–6 and 8, related to Figure 3. The matrix shows inferred introgression proportions as estimated from gene tree counts for the introgressed species pairs (STAR Methods), and then mapped to internal branches using the *f*-branch method. The expanded tree at the top of each matrix shows both terminal and ancestral branches. The tree on the left side of each matrix represents species relationships with mapped introgression events (red arrows) derived from the corresponding *f*-branch matrix (STAR Methods). The fractions next to each arrow represent the number of triplets that support a specific introgression event by both DCT and BLT divided by the total number of triplets that could have detected the introgression event. Dashed arrows represent introgression events with low support (triplet support ratio < 10%). Clades 1 and 3 are not shown because no introgression was found in these clades according to the DCT-BLT combined test.

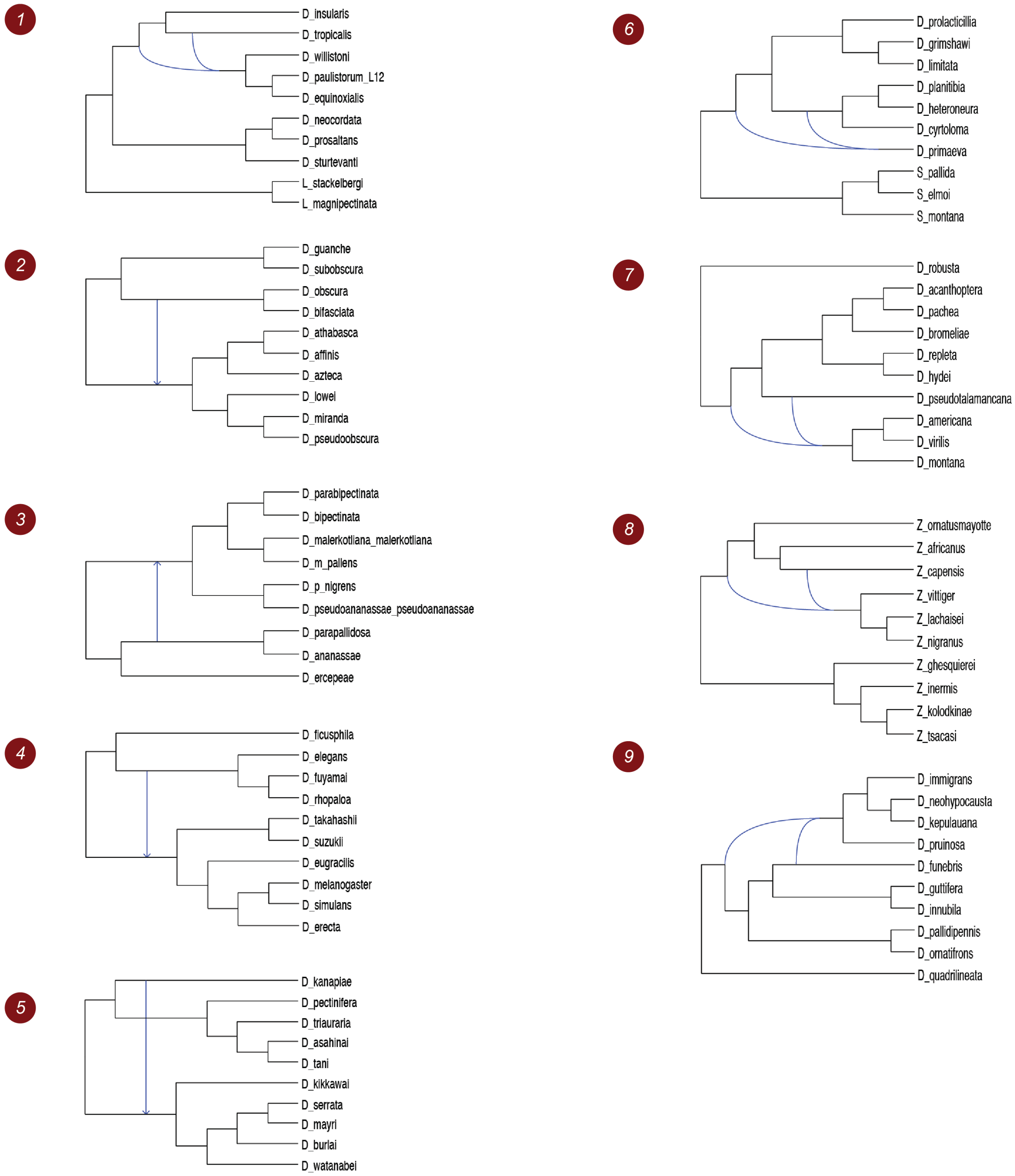

Figure S4. Patterns of introgression inferred for the monophyletic clades 1–9 using PhyloNet, related to Figure 3. For each clade we show the topology of the phylogenetic network with the highest likelihood. Blue branches denote reticulations. Note that for all clades except clade 8, the networks with the highest likelihood scores from PhyloNet qualitatively agree with the inferred introgression patterns by the DCT-BLT results summarized by `Dsuite`: the best-supported position of a reticulation event inferred by PhyloNet tended to occur in the same or similar locations on the tree as introgression events we inferred with our DCT-BLT analysis. On the other hand, PhyloNet inferred an introgression event in clade 8 that is more ancient than that inferred by DCT-BLT (an introgression event between *Z. capensis* and the *Z. camerounensis*-*Z. nigranus* ancestor detected by DCT-BLT is pushed back to the *Z. camerounensis*-*Z. vittiger* ancestor by `PhyloNet`). Uncertainty over the precise history of introgression in clade 8 notwithstanding, PhyloNet is consistent with our DCT-BCT analysis and identifies introgression across the *Drosophila* phylogeny.

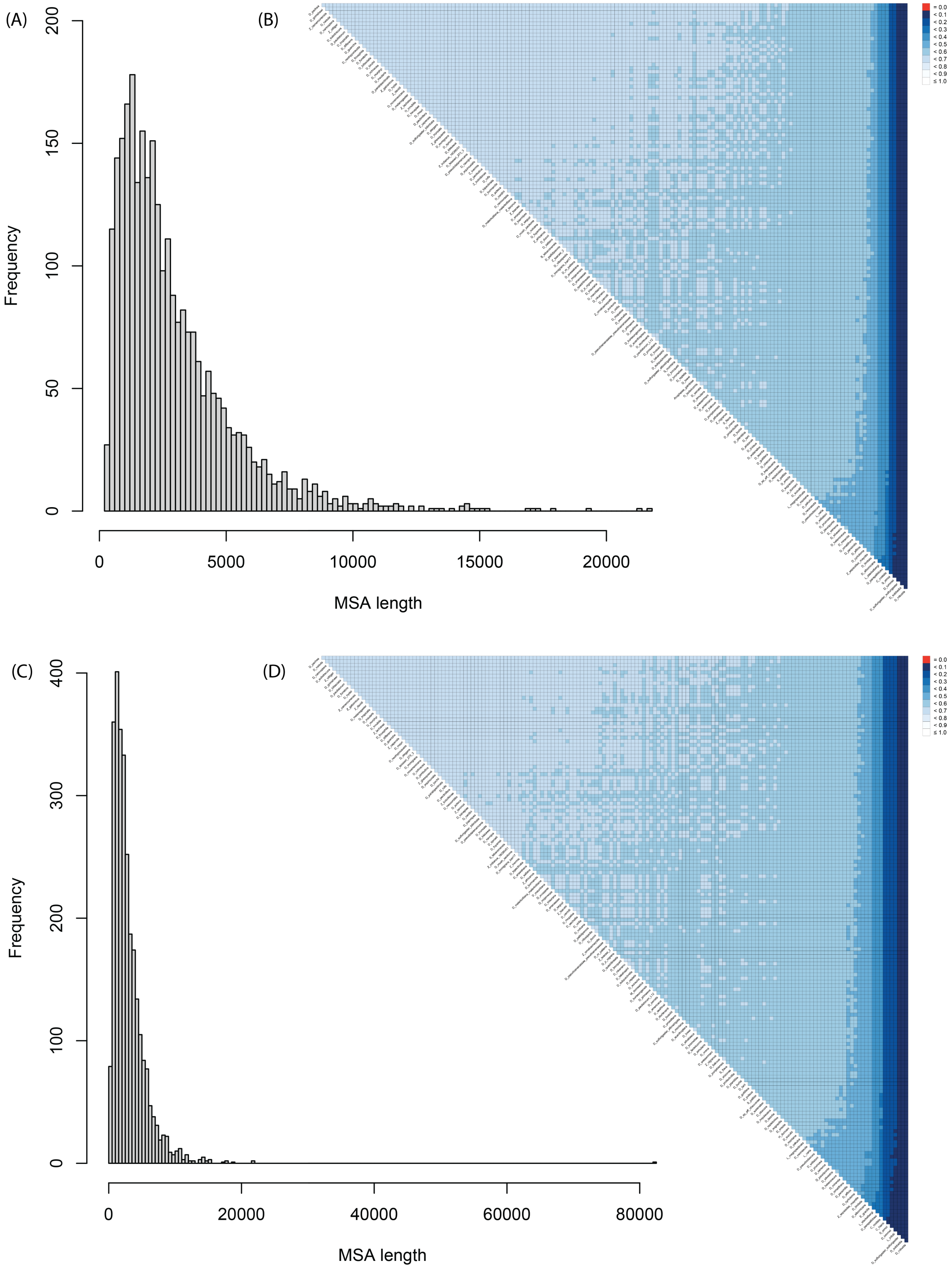
(A)
Frequency
0
50
100
150
200
MSA length
0
5000
10000
15000
20000
(B)
= 0.0
< 0.1
< 0.2
< 0.3
< 0.4
< 0.5
< 0.6
< 0.7
< 0.8
< 0.9
≤ 1.0
(C)
Frequency
0
100
200
300
400
MSA length
0
20000
40000
60000
80000
(D)
= 0.0
< 0.1
< 0.2
< 0.3
< 0.4
< 0.5
< 0.6
< 0.7
< 0.8
< 0.9
≤ 1.0

Figure S5. Supermatrix completeness scores and distribution of BUSCO MSA lengths, related to Figure 1. Matrices show pairwise completeness metric values computed by AliStat (the fraction of sites for which both sequences have a completely specified character). Larger values indicate higher levels of MSA completeness. MSA length distributions and AliStats matrices were generated for datasets where *Anopheles gambiae* (panels A and B) and *Musca domestica* (panels C and D) were used as outgroups.

	BLT (%)	DCT (%)	DCT-BLT (%)
Excluded alignments < 1000 bp	84	94	80
Consistent Muller element	70	89	76
d_N/d_S filter	69	82	54
Random subsampling	76	85	65
TreeShrink	75	66	52

Table S1. Summary table for the robustness of the introgression analysis results to data quality and evolutionary rate, related to Figure 3. Percentages indicate how many introgressing pairs of species identified by BLT, DCT and their intersection after applying different filters overlap with the introgression pairs identified without applying them.

Performance evaluation of BLT and DCT analyses on gene trees that excluded alignments with fewer than 1,000 sites (the "Excluded alignments < 1000 bp" row above): A large fraction of introgressing species pairs that were identified by BLT, DCT, and their intersection remained significant after filtering out these short alignments (Data S2).

Impact of rapid karyotype evolution observed in the *obscura* group (clade 2) on introgression inference ("Consistent Muller element"): Loci that did not belong to the same Muller element within all three species examined in a triplet were excluded before repeating our BLT-DCT analysis on clade 2. This filtering scheme had only a minor impact on introgression estimation after filtering out loci that are found on different Muller elements in species within this clade (Data S2). More importantly, this filtering had no impact on the introgression events discussed below and shown in Figure 2—the exact same events were inferred for clade 2.

Effects of evolutionary rate (as measured by d_N/d_S) heterogeneity across branches on introgression inference ("d_N/d_S filter"): For each triplet tested by BLT and DCT, gene trees with $d_N/d_S > 0.53$ were excluded; this cutoff corresponds to the upper 5% critical value of d_N/d_S distribution across all the clades and gene trees. Importantly, a large number of genes are removed when applying this filter because only one branch within the portion of the gene tree relevant to the triplet must exceed the critical value of d_N/d_S to result in the entire gene tree's removal (Data S2). We therefore asked to what extent this reduced fraction of introgressing taxon pairs is a consequence of reduced power due to the reduction in the number of gene trees ("Random subsampling"). We found that randomly subsampling gene trees without respect to d_N/d_S value can affect introgression inferences in a similar fashion (see STAR Methods). Although we don't rule out the possibility that evolutionary rate heterogeneity may influence our DCT-BLT analysis, e.g. 54% of DCT-BLT results is significantly different ($P < 0.001$) from the mean (66%) of distribution of percentages obtained by repeating resampling procedure 1000 times, or that the persistence of introgressed alleles may be correlated with a gene's evolutionary rate, this result shows that our estimates of gene flow are not being driven primarily by genes evolving under the least amount of selective constraint and/or the greatest amount of positive selection.

Performance of BLT and DCT using a gene tree set with potentially misaligned sequences removed ("TreeShrink"): After using TreeShrink to remove potentially misaligned sequences, we obtained results largely concordant with other methods as shown in Data S2. However, we notice several exceptions: in clades 5 and 7 the number of species pairs with at least one triplet that is significant according to both the DCT and BLT methods is markedly higher after running TreeShrink, largely due to an increase in significant DCT results. Conversely, for Hawaiian drosophilids (clade 6) we no longer observe any overlap between triplets identified by BLT and DCT after filtering via TreeShrink.

Clade	Introgression Event
2	*D. obscura…D. bifasciata* ⟷ *D. pseudoobscura…D. affinis*
4	*D. erecta...D. orena* ⟷ *D. mauritiana...D. melanogaster*
4	*D. ficusphila* ⟷ *D. carrolli…D. elegans*
7	*D. robusta* ⟷ *D. pseudotalamancana*
7	*D. robusta* ⟷ *D. americana...D. montana*
7	*D. hydei* ⟷ *D. arizonae...D. seriema*
7	*D. pseudotalamancana* ⟷ *D. americana...D. montana*
7	*D. pachea* ⟷ *D. acanthoptera*
7	*D. novamexicana* ⟷ *D. arizonae...D. hydei*
7	*D. hydei* ⟷ *D. americana...D. novamexicana*
7	*D. americana...D. novamexicana* ⟷ *D. arizonae...D. seriema*
9	*D. funebris...D. mush sãotomé* ⟷ *D. albomicans…D. pruinosa*
9	*D. pruinosa* ⟷ *D. arawakana...D. mush sãotomé*

Table S2. Introgression scenarios estimated by the stringent version of DCT-BLT approach, related to Figure 3. Here we applied a more stringent version of the DCT-BLT that compares the branch lengths of the discordant topology with those of the concordant topology and is thus not sensitive to ancestral population structure (Method Details). Of the 511 triplets that were significant according to our combined DCT-BLT test, 144 (28.1%) remain significant when imposing this much more stringent version of the BLT (again, after FDR correction). We then asked how many of the 30 introgression events shown in Figs. 3 and S3 were significant by this more stringent test for at least one triplet, finding that 13 of the 30 events (43.3%) are significant, including 11/17 (64.7%) of the most strongly supported events (those significant in at least 10% of triplets in our original analysis and shown in solid lines in Figs. 3 and S3).

Supplemental References

S1. Grimaldi, D., and Engel M.S. (2005). Evolution of the Insects. Cambridge University Press, New York and Cambridge.

S2. Winkler, I.S., Labandeira, C.C., Wappler, T., Wilf, P. (2010). Distinguishing Agromyzidae (Diptera) Leaf Mines in the Fossil Record: New Taxa from the Paleogene of North America and Germany and Their Evolutionary Implications. Journal of Paleontology 84, 935–954.

S3. von Tschirnhaus M., Hoffeins C. (2009). Fossil flies in Baltic amber—Insights in the diversity of Tertiary Acalyptratae (Diptera, Schizophora), with new morphological characters and a key based on 1000 collected inclusions. Denisia 26:171.

S4. Grimaldi, D.A. (1987). Amber fossil Drosophilidae (Diptera), with particular reference to the Hispaniolan taxa. American Museum novitates ; no. 2880. Amber drosophilids.

S5. Russo, C.A.M., Mello, B., Frazão, A., Voloch, C.M. (2013). Phylogenetic analysis and a time tree for a large drosophilid data set (Diptera: Drosophilidae). Zoological Journal of the Linnean Society 169, 765–775